DESIGN OF AN ACCELERATING STRUCTURE
FOR A 500 GeV CLIC USING ACE3P*

Kyrre Ness Sjobak[†] and Erik Adli, Department of Physics, University of Oslo, Norway
Alexej Grudiev and Walter Wuensch, CERN, Geneva, Switzerland

Abstract

An optimized design of the main linac accelerating structure for a 500 GeV first stage of CLIC is presented. A similar long-range wakefield suppression scheme as for 3 TeV CLIC based on heavy waveguide damping is adopted. The accelerating gradient for the lower energy machine is 80 MV/m. The 500 GeV design has larger aperture radius in order to increase the maximum bunch charge and length which is limited by the short-range wakefields. The cell geometries have been optimized using a new parametric optimizer for Ace3P and details of the RF cell design are described. Field parameters for the full structure are calculated using a power flow equation.

INTRODUCTION

One of the design options for the CLIC (Compact LInear Collider) is to first build a machine capable of 500 GeV center of mass energy, which can later be expanded to 3 TeV. The optimal accelerating structure for a 500 GeV accelerator is slightly different from the current 3 TeV design CLIC_G [2], even if the topology is shared. This is due to a higher bunch charge, partly compensated by relaxing the transverse wakefield limit due to the shorter linac length.

This paper presents a RF design for the structure CLIC_502, which is optimized for operation in a 500 GeV CLIC. The detail of the geometry and RF computations is at a level where it is soon possible to build a prototype of the structure, which was originally presented in an earlier design stage at LINAC'10 [1].

DESIGN OF SINGLE CELLS

The geometry of three single cells named "first", "middle", and "last" was varied using the parameters shown in Fig. 1 in order to minimize the peak surface field to gradient ratios. The iris aperture radius **a** and thickness **d** were fixed based on short range wake field limits, while the outer wall parameters **eow**, **c**, and iris parameters **e** and **sFrac** were varied. For each of these combination of parameters, the cell radius **b** was tuned in order to have the correct frequency $f_0 = 11.994$ GHz for the TM_{01}-like mode at 150° RF phase advance per cell. The final design of these single cells were then combined in order to get the full structure, as described in the next section.

The calculation of the surface fields and other RF parameters were made using the finite element eigenmode solver Omega3P [4]. An separate program, AcdOptiGui [5], was used to steer the calculations and post-processing. The
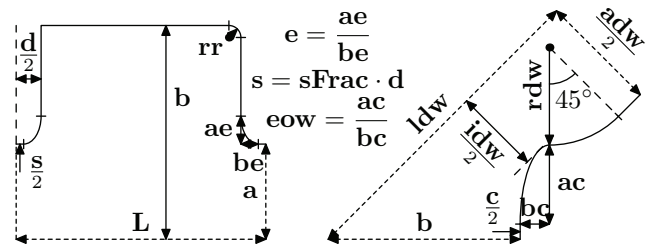
Figure 1: Geometry parameters for the single cells, showing iris parameters (left) and outer wall/damping waveguide parameters (right). The damping waveguide transverse dimensions are **idw** = 8.0 mm and **adw** = 11.0 mm.

setup and benchmarking of Omega3P and post-processing is described in [6]. All calculations were by default run with 2nd order tetrahedral Nedelec elements for the electric field, and 1st order for the magnetic field (E-formulation). In cases of doubtful convergence the calculation was rerun with a denser surface mesh in the problematic areas, using both the E-formulation and also switching the electric and magnetic element orders (H-formulation). When multiple simulation results for the same geometry were available, non-converged results showing extremely high local field values were discarded, and the remaining results were averaged. Simulation results where $\Delta f = |f - f_0| > 10$ MHz were also discarded, only keeping geometries with the right frequency.
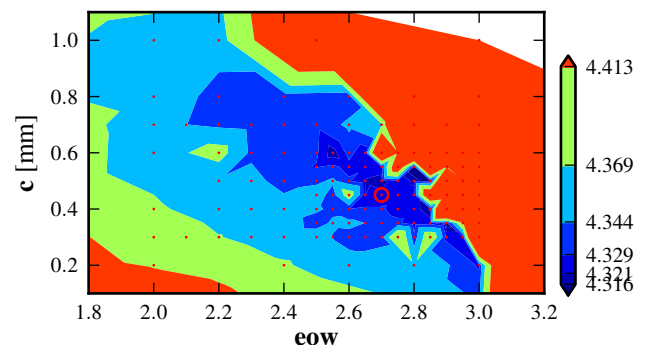

Figure 2: $|H|^{\mathrm{surf}}/E_{\mathrm{acc}}$ in mA/V for the last cell. Calculated points in red, chosen parameters marked by red circle.

For each cell, the outer wall parameters was varied first in order to minimize peak surface magnetic field. In order to keep the right frequency, some points in the region of interest were first selected and tuned to the right radius by changing the radius **b**. Having these points, **b** was then fitted as a quadratic function of (**eow**,**c**), and this function then used to predict the radius for following (**eow**,**c**) points. The accumulated simulation results were then plotted as shown in Fig. 2, and an approximate minimum selected.

After fixing the outer wall parameters, iris parameters

were similarly varied in order to minimize the peak surface electric field and the modified Poynting vector S_c [3]. It was quickly found that these fields were very weak functions of **sFrac**, which was therefore locked at a small value. The relative deviations from the minimum fields were then plotted as for the outer wall, and an approximate optimum taking both minima into account selected.

Having the final geometry parameters for a cell, several calculations with different mesh using both E- and H-formulation were performed in order to check convergence. The means of the resulting field parameters from these calculations were taken as the final value for the field parameters, and the error estimate used was $\pm 1.96 \cdot \sqrt{\text{variance}/n}$. The results are shown in Table 2.

In all cells the magnetic field as a function of the outer wall parameters had a similar structure as the one shown in Fig. 2, with a broad minimum depending on both parameters. A set of parameter values were first chosen for the first and last cell, using the same value for **eow** but different values of **c**, and avoiding the region of rapid rise in the upper-right corner of the plot, which is due to field concentration on the damping waveguide entrances.

For the irises, both the electric field and S_c were roughly parabolic functions of **e**, with the electric field smallest for smaller values of **e** than S_c. This is due to the electric field being largest in the case of a "pointy" iris, while S_c grows if the electric field is spread into the regions where the magnetic field is non-negligible. It was also seen that the minimum S_c was lower for smaller iris apertures which has longer iris to outer wall distance.

For the middle cell, it was chosen to set all parameters except **b** as the average between the first and last cell. This choice was verified by varying the parameters, and found satisfactory. This makes the tapering linear, making for a less complicated full structure geometry.

FIELDS IN COMPLETE STRUCTURE

The data for the three single cells described above was used to interpolate their relative field parameters along a complete structure, which was then used to calculate the power flow and absolute fields, using a continuous analytic approach for the steady-state fields [7]. The relative fields at $z = 0$ was fixed at the parameters for the "first" cell, the fields at $z = N_{\text{cells}} \cdot \mathbf{L}$ at the "last" cell parameters, and $z = \frac{N_{\text{cells}} \cdot \mathbf{L}}{2}$ at the "middle" cell, where N_{cells} is the number of cells for the structure.

The pulsed surface heating temperature increase was calculated using Equation (3.36) and OFE copper data from [8], describing the temperature increase due to surface currents induced by RF pulses on the surface of a relatively flat and thick conductor. The assumed pulse was piecewise linear in power, with first a linear rise from $P = 0$ to P_{rise} in time $t_{\text{rise}} = 15.3ns$, followed by continued increase to P_{in} in time $t_{\text{fill}} = \int_0^L \frac{\mathrm{d}z'}{v_g(z')}$, flat-top of length $t_{\text{beam}} = t_{\text{bunch}} \cdot N_{\text{bunches}}$, linear decline to P_{rise} in t_{fill}, and finally decline to $P = 0$ in t_{fill}. Here t_{rise} was assumed

Table 1: Full Structure RF and Pulse Parameters

Number of cells N_{cells}	22	
Active length	229	mm
Peak/steady-state P_{in}	74.2	MW
Average loaded E_{acc}	80	MV/m
$\max(|E|_{\text{loaded}}^{\text{surf}})$	217	MV/m
$\max(|E|_{\text{unloaded}}^{\text{surf}})$	227	MV/m
$\max(\Delta T_{\text{loaded}})$	41	K
$\max(\Delta T_{\text{unloaded}})$	46	K
$\max(S_c)$	4.61	MW/μm^2
RF $\rightarrow$ beam efficiency η	39.6	%
t_{fill}	48.0	ns
Bunch separation t_{bunch}	0.5	ns
N_{bunches}	354	
Bunch population $N_{\text{particles}}$	$6.8 \cdot 10^9$	$e^\pm$

to be the same as in [1], and P_{rise} as the power at the beginning of the beam-loading compensation ramp described in [7].

The number of cells was assumed to be 22, such that the structure length would be the approximately equal to [1]. We see that the RF parameters found are more-or-less identical to what were found here, except for ΔT. The increase in number of regular cells is possible because this structure is likely to be built with compact couplers, where the end cells also couple the power in and out of the structure. These cells are assumed to have similar properties as regular cells, and should thus not make a large difference on the RF parameters.
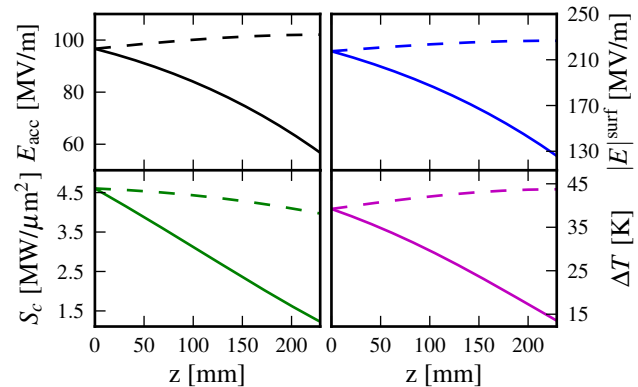
Figure 3: The new structure's gradient and peak fields at flattop, and peak temperature increase along structure in loaded (continuous lines) and unloaded (dashed) case.

The final result is clearly within RF constraints of $\max(|E|^{surf}) < 260$ MV/m and $\max(\Delta T) < 56$ K [1]. Comparing to CLIC_G which has $\max(S_c) = 5.7 \frac{\text{MW}}{\mu m^2}$ and $P/C = P/(2\pi\mathbf{a}) = 3.10$ MW/mm at first iris, CLIC_502 reaches lower values, with $P/C = 2.97$ MW/mm.

WAKEFIELDS

The maximum permitted single-bunch transverse wakefield at the 2nd bunch is given by $W_{\perp,2}^{\max} \cdot N_{\text{particles}} = \frac{C \times 4 \cdot 10^9 E_{\text{acc}}}{150[\text{MV/m}]}$, where the constant C is increased from 10 V/pC/mm/m for the 3 TeV case to 20 V/pC/mm/m due to

07 Accelerator Technology and Main Systems

T06 Room Temperature RF

Table 2: Single Cell Geometry and Field Parameters with 95% stat. Confidence Intervals for Field Parameters

|		First	Middle	Last	
Period	**L**	10.41467	10.41467	10.41467	mm
Iris aperture radius	**a**	3.97	3.625	3.28	mm
Iris thickness	**d**	2.08	1.875	1.67	mm
Outer wall ellipticity	**eow**	2.7	2.7	2.7	-
Outer wall flat length	**c**	0.7	0.575	0.45	mm
Iris flat frac.	**sFrac**	0.01	0.01	0.01	-
Iris ellipticity	**e**	1.6	1.65	1.7	-
Cell radius	**b**	8.9161	8.765469	8.63023	mm
Frequency		$11.993916\pm8\times10^{-6}$	$11.993975\pm2\times10^{-6}$	$11.993984\pm4\times10^{-6}$	GHz
Q-factor		6364.8 ± 0.9	6370.5 ± 0.6	6383 ± 1	-
$(R/Q)/\mathbf{L}$		10304.92 ± 0.06	11213.4 ± 0.2	12175.9 ± 0.2	Ω/m
v_g		2.056 ± 0.004	1.614 ± 0.002	1.234 ± 0.003	c (%)
$\max(|H|^{\mathrm{surf}})/E_{\mathrm{acc}}$		4.684 ± 0.003	4.511 ± 0.003	4.342 ± 0.002	mA/V
$\max(|E|^{\mathrm{surf}})/E_{\mathrm{acc}}$		2.25 ± 0.06	2.23 ± 0.03	2.22 ± 0.06	-
$\max(S_c)/E_{\mathrm{acc}}^2$		0.493 ± 0.003	0.435 ± 0.001	0.381 ± 0.001	mA/V
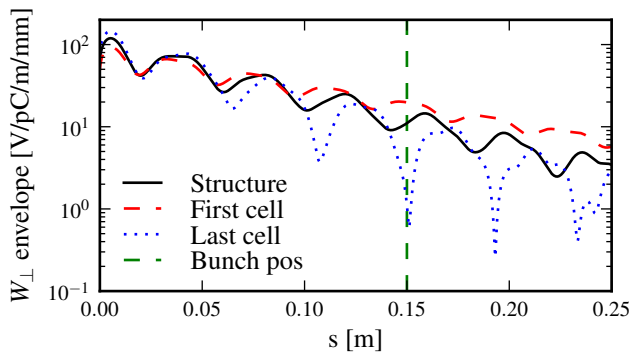
Figure 4: Envelope of estimated transverse wakefield.

shorter linac length. The maximum permitted wake is thus $W_{\perp,2}^{\max}$ = 6.3 V/pC/mm/m.

A preliminary study of the transverse wakefields was done by simulating the wake generated by the first and last cells using T3P [4], and fitting the two first modes in the impedance spectras to get the frequency, Q-factor, and amplitude of the modes. These values were then interpolated linearly to estimate the wake parameters for the remaining 20 cells, and the total wake found by summing over these partial wakes. The resulting wake envelope is shown in Figure 4, and the estimated wake envelope at 2nd bunch is 11 V/pC/mm/m.

This is above the stated limit, and indicates that the damping waveguide entrance width **idw** should be increased to couple out the dipole modes more efficiently, requiring a partial re-optimization of the single cells.

However, it should be noted that the simulation results might not be completely converged. A convergence study of T3P was done comparing it to GdfidL results for a similar geometry, showing that absorbing boundary conditions at the end of the damping waveguides where not sufficient, and that waveguide boundary conditions were necessary for convergence. However, at the time of writing there were some problems getting T3P to work reliably with the number of separate damping waveguides needed.

CONCLUSIONS

The design of the CLIC_502 accelerating structure has been refined to a higher detail level. Most of the RF parameters are close to what was found by the initial study [1], except ΔT. An early estimate of the wakefields in the structure has also been done, indicating that the damping might need to be increased. Finally, a parametric interface and data management program for Omega3P was developed, improving the workflow for geometry optimization using Omega3P.

ACKNOWLEDGMENT

REFERENCES

[1] A. Grudiev and D. Schulte, "THE ACCELERATING STRUCTURE FOR A 500 GEV CLIC," LINAC'10, Tsukuba, September 2010.

[2] A. Grudiev, W. Wuensch, "DESIGN OF THE CLIC MAIN LINAC ACCELERATING STRUCTURE FOR CLIC CONCEPTUAL DESIGN REPORT," LINAC'10, Tsukuba.

[3] A. Grudiev, S. Calatroni and W. Wuensch, "New local field quantity describing the high gradient limit of accelerating structures," Phys. Rev. ST Accel. Beams 12, 102001 (2009).

[4] K. Ko et al, "Advances in Parallel Electromagnetic Codes for Accelerator Science and Development," LINAC'10, Tsukuba

[5] https://github.com/kyrsjo/AcdOpti

[6] CERN EDMS document no. 1166750 v.2,

[7] A. Lunin, V. Yakovlev and A. Grudiev, "Analytical solutions for transient and steady state beam loading in arbitrary traveling wave accelerating structures," Phys. Rev. ST Accel. Beams 14, 052001 (2011).

[8] David P. Pritzkau, "RF Pulsed Heating," SLAC report 577.